

# Re-configurable multi-level temperature sensing by ultrasonic “spring-like” helical waveguide

Suresh Periyannan, Prabhu Rajagopal, and Krishnan Balasubramaniam

Citation: *J. Appl. Phys.* **119**, 144502 (2016); doi: 10.1063/1.4945322

View online: <http://dx.doi.org/10.1063/1.4945322>

View Table of Contents: <http://aip.scitation.org/toc/jap/119/14>

Published by the [American Institute of Physics](#)

---

---

# Re-configurable multi-level temperature sensing by ultrasonic “spring-like” helical waveguide

Suresh Periyannan, Prabhu Rajagopal, and Krishnan Balasubramaniam<sup>a)</sup>

*Centre for Non Destructive Evaluation and Department of Mechanical Engineering,  
Indian Institute of Technology Madras, Chennai 600 036, India*

(Received 22 November 2015; accepted 21 March 2016; published online 13 April 2016)

This paper introduces a novel technique for multi-level temperature measurement using a single reconfigurable ultrasonic wire waveguide that is configured in the form of a helical spring. In this embodiment, the multiple sensing levels located along the length of the helical waveguide wire can be repositioned by stretching or collapsing the spring to provide measurements at different desired spacing in a given area/volume. This method can measure over a wide range of temperatures. The transduction is performed using Piezo-electric crystals that are attached to one end of the waveguide which act as transmitter as well as receiver. The wire will have multiple reflector embodiments (notches was used here) that allow reflections of input L(0,1) mode guided ultrasonic wave, in pulse echo mode, back to the crystal. Using the time of flight measurement at multiple predefined reflector locations, the local average temperatures are measured and compared with co-located thermocouples. The finite element modeling simulation was used to study the effect of excitation frequency and the mean coil diameter of the “spring-like” waveguide. This technique improves on the limitations of a straight waveguide technique earlier reported. © 2016 AIP Publishing LLC.

[<http://dx.doi.org/10.1063/1.4945322>]

## I. INTRODUCTION

The development of an ultrasonic temperature sensor is motivated by many temperature profile measurement requirements in industries, such as glass and metal melting plants, process industries, and nuclear power plants, where temperature control is critical. In order to control the industrial processes, it is required to continuously or periodically monitor the temperatures at multiple levels inside a high temperature environment. Periyannan and Balasubramaniam<sup>1</sup> have reported a multiple ultrasonic waveguide system, made of Chromel material, for the temperature measurements at multi levels in a Joule melter using L(0, 1) guided wave mode using a bank of straight waveguides. Other efforts on the measurement of temperature and rheological properties of molten glass have been reported elsewhere, where the Time of Flight (TOF) and amplitude (A) of the reflected ultrasonic signal received at one end of a waveguide were used in the measurement while the other end was immersed in the molten material.<sup>2–8</sup> Pandey *et al.*<sup>9</sup> demonstrated that, using the ultrasonic guided flexural mode F(1, 1) in a long buffer rod, the rheological properties of mould powder slags during the steel billet casting process could be measured over a range of temperatures up to 1100 °C. In a similar work using cladded waveguides, Jen *et al.*<sup>10</sup> demonstrated the on-line monitoring of curing of polymers inside moulds at elevated temperatures.

Thermocouple and radiation pyrometers are common temperature sensors used for temperature measurement in the industry. However, these diagnostic tools have issues while being used in the industry. The pyrometers require a line-of-sight that is often not feasible in several enclosed industrial

high temperature processes. The thermocouples and RTDs often suffer due to sensor drift during long term operation, as reported elsewhere by Bentley.<sup>11</sup> The footprint of a thermocouple (involving two wires and often ceramic coatings/beads), flexibility of these wires, and its ability to measure temperature only in one location, etc., are all considered as limiting factors for industrial applications where temperatures at different locations must be monitored. Additionally, the failure of the junction in a thermocouple is of concern, particularly for high temperature operations. Hence, alternate multi-level sensing technologies that are more robust and have smaller footprint is desirable. Ultrasonic waveguide technique has the potential to address some of these limitations.

Several waveguide based ultrasonic sensing of temperature, viscosity, corrosion, etc., have been recently reported in the literature. Huang *et al.*<sup>12</sup> and Tsai *et al.*<sup>13</sup> proposed an ultrasonic system for air temperature measurement using changes in the speed of sound calculated from phase shift records; a similar concept was used to measure temperature by Zhan *et al.*<sup>14</sup> Using a bent waveguide that is surrounded by a fluid, with known properties (such as air), the elastic moduli of the waveguide was obtained at different temperatures by Periyannan and Balasubramaniam.<sup>15–17</sup> Cawley and Cegla<sup>18</sup> have developed an ultrasonic instrument using a thin elongated strip to separate the transducer from a potentially hostile environment associated with the object under test for thickness measurements. Other efforts include liquid level and temperature monitoring using single torsional acoustic waveguide (TAW) approach<sup>19</sup> as well as liquid level in wine bottles.<sup>20</sup>

Most of the previous approaches described measurements in a single zone of interest. In order to measure at multiple points of interest using a single waveguide, Visvanathan and Balasubramaniam<sup>21</sup> had described the monitoring of a moving

<sup>a)</sup>Author to whom correspondence should be addressed. Electronic mail: [balas@iitm.ac.in](mailto:balas@iitm.ac.in). Telephone: 044-22575688.

air-to-fluid interface signal during a resin filling process inside an opaque model and obtained the dynamics of the resin flow front.

Here, we explore the feasibility of using multiple “notch” embodiments as reflectors that are positioned along the length of the waveguide and their ability in making multiple measurements using a single ultrasonic probe. Additionally, the configuration is a helical “spring like” waveguide that allows for the flexibility of making measurements at locations that are very close to each other (by reducing the helix angle) or in a relatively sparse spacing (by increasing the helix angle). In this work, the temperature measurements at multi levels in a furnace using such a reconfigurable waveguide is discussed and demonstrated.

The ultrasonic waveguide-based temperature sensing approaches have several advantages over the conventional thermocouples. This includes the inherent property of higher reliability since there is no junction that can fail, as well as the ability to program several zones of measurements in one waveguide. In this paper, the authors aim to measure the temperatures at different depths of hot regions using multiple embodiments in a single waveguide system. The finite element modeling (FEM) simulations were employed in order to select the wire diameter and the diameter of the helix. Then, the sensor was evaluated in laboratory conditions by placing the sensor inside a furnace with uniform and varying temperature regions. The re-configurability of these sensors was also demonstrated by using the same waveguide in two different configurations by changing the pitch between the sensor locations (consequently changing the helix angle).

## II. BACKGROUND

### A. Waveguide temperature sensors

Waveguide temperature sensors measure changes in time of flight of an ultrasonic wave mode due to the changes in the material properties of the waveguide ( $l$ ,  $\alpha$ ,  $E$ ,  $G$ , and  $\rho$ ) as a function of temperature.<sup>1</sup> Here,  $l$  is the gage length,  $\alpha$  is the coefficient of thermal expansion,  $E$  and  $G$  are the elastic moduli, and  $\rho$  is the mass density. In order to localize the measurement, embodiments such as notches, bends, and gratings can be introduced in the waveguide that allow for the signals to be reflected from these embodiments. The gage length of measurement would be the region in-between any two embodiments. The measurement of the relative time of flight (TOF) between these reflections can be monitored and used to obtain the average temperature of in-between the two reflectors. For a reliable TOF measurement, the reflected signals must be time resolved and identified for which the spacing between the embodiments must be optimized. For a straight waveguide, the gage length is pre-determined and often will be of the order of 30–40 mm. Also, the measurement will be an averaged TOF over this gage length. Figure 1 compares the straight waveguide with a comparable helical “spring-like” waveguide. Periodically spaced notches are introduced in the waveguides that provide reflected signals from these locations. The difference in TOF between any two reflections can be used to determine the average temperature of the waveguide material, and consequently the

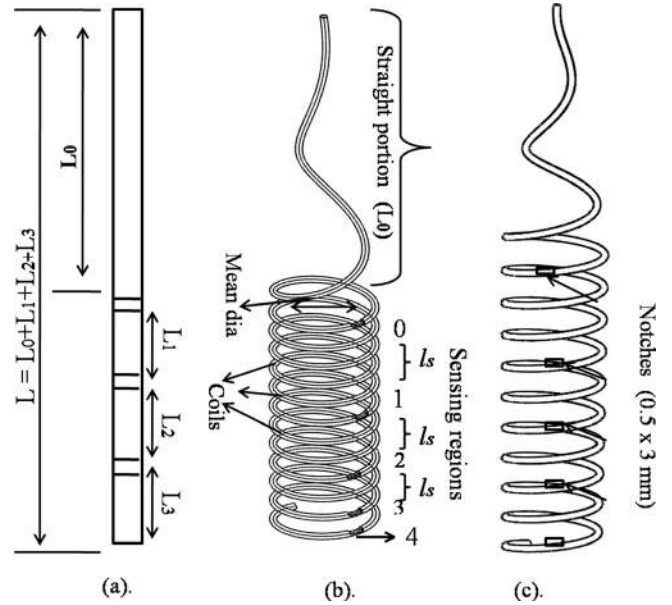


FIG. 1. Illustration of temperature gradient measurement concept in (a) straight waveguide, (b) and (c) Helical waveguides.

temperature of the surrounding medium, in the region in between the notches. In Figures 1(b) and 1(c), the helical waveguide is illustrated in two possible helix angle configurations (achieved by changing the pitch between sensors). The compressed position in Figure 1(b) allows for temperature measurements that are relatively closely spaced compared to the straight waveguide shown in Figure 1(a). Figure 1(c) shows that the helical waveguide can be reconfigured to measure at points similar to the straight waveguide by stretching the waveguide. The difference in the time of flight between the received signals from the notches can be expressed as

$$(\delta\text{TOF})_{\text{helical}} = \left(\frac{L_n}{C_n}\right)_{T_i} - \left(\frac{L_n}{C_0}\right)_{T_0} = (\text{TOF})_i - (\text{TOF})_0 \quad (1)$$

$$\begin{aligned} \text{Running length of the wire } (L) &= \Sigma L_n \\ &= L_0 + L_1 + L_2 + L_3 + \dots \quad (n = 0, 1, 2, \dots) \quad (2) \end{aligned}$$

$$\begin{aligned} \text{Free length of helical waveguide } (l) &= \Sigma l_s \\ &= l_0 + l_1 + l_2 + l_3 + \dots \quad (s = 0, 1, 2, \dots) \quad (2a) \end{aligned}$$

$l_s < L_n$ , for helical waveguide and  $l_s = L_n$  only for a straight waveguide (Figs. 1(a) and 1(b)) where  $C_0$  = Wave velocity in the waveguide at room temperature ( $T_0$ ),  $C_n$  = Wave velocity in the waveguide section ( $L_n$ ) at instantaneous temperature ( $T_i$ ),  $L_0, L_1, L_2, \dots$  are wire lengths (in straight or helical waveguide) between two notches (Figs. 1–3),  $l_s$  = Length of each sensing portion.

The design of the helical waveguide can be modified by (a) increasing the number of active coils, (b) adjusting the mean coil diameter, and (c) altering the helix angle and thereby changing the relative spacing between the embodiments (i.e., pitch between the sensors). In this paper, notches type of embodiments (0.5 mm deep and 3 mm long) were

machined along the length of the 1.18 mm diameter waveguide to provide reflected signals from each embodiment. Hence, the sensing region and the spacing between the measurements may be adjusted in the radial as well as the axial directions (1D, 2D, or 3D) based on requirements and appropriate waveguide design.

### B. Ultrasonic waves in “spring-like” helical wire waveguide

The guided waves can be thought of as a superposition of partial plane wave modes that constructively interfere within waveguide boundaries.<sup>22</sup> The propagation of ultrasonic waves in waveguides is characterized by variables, namely, frequency, phase velocity, and attenuation. In a cylindrical waveguide, there are three families of modes: longitudinal (L), torsional (T), and flexural (F) that are propagating in the axial direction ( $z$ ) of cylindrical coordinate system ( $r$ ,  $\theta$ , and  $z$ ).

While, many wave modes can be excited in cylindrical rods, in this paper, we will concentrate on the fundamental longitudinal mode,  $L(0, 1)$ . This mode has smaller levels of dispersion over a wide range of frequencies (0–500 kHz) for the range of high temperature materials of interest here, as listed in Table I. The phase velocity dispersion curves for the two fundamental axi-symmetric modes  $L(0,1)$  and  $T(0,1)$  obtained using DISPERSE,<sup>23</sup> for a typical high temperature material waveguide (Chromel) are shown in Figure 2(a). It is desirable that, in the chosen frequency range, the waveguide thickness must exhibit only a small degree of dispersion. This ensures that the pulse width of the signals remains relatively unchanged and thus improves the TOF measurements. Here, an operational frequency range of 200–500 kHz was chosen. Further, in order to ensure low dispersion, at an appropriate thickness of the wire, the suitable mean coil diameter (helix diameter) was selected using FEM simulations as described later in Section III.

The studies on waves in helical waveguides have been reported on electromagnetic waves<sup>24</sup> and elastic waves for structural health monitoring<sup>25</sup> with applications in civil structures. The elastic wave dispersion effects were modeled using a Semi-Analytical Finite Element (SAFE) method using a non-orthonormal coordinate system that is aligned along an arbitrary cross-section of the helical waveguide. All three types of wave modes, that is,  $L(n, m)$ ,  $T(n, m)$ , and  $F(n, m)$  that are supported in a waveguide were considered and analyzed.<sup>25</sup>

### III. HELICAL WAVEGUIDE DESIGN USING FINITE ELEMENT MODELING

The waveguide diameter ( $d$ ) was chosen based on the dispersion curve analysis and availability of Chromel wire. Based on elasto-dynamic FEM model, using commercial

software ABAQUS<sup>®</sup> 6.11 platform, simulation studies were performed on the wave propagation in the rods and tubes in order to obtain the predicted displacement response.<sup>26</sup> The wave propagation simulations were performed for a pulse-echo mode measurement using Chromel helical waveguides. The material properties, the FEM model details, etc., used in the simulations are listed in Table I. The Elastic Moduli of the waveguide material were obtained using two measurements of velocities of the  $L(0,1)$  wave mode and the  $T(0,1)$  wave mode as explained elsewhere<sup>15,27</sup> and the density of the material was measured using the mass and volume measurements.

In this experiment the Chromel waveguide, in a straight configuration, was employed and the velocities obtained experimentally were  $V_g$  for  $L(0,1) = 4980$  m/s and  $V_g$  for  $T(0,1) = 3080$  m/s at room temperature. The A-scan signals were obtained by plotting the displacements at the receiver nodes as a function of time. The receiver nodes coincide with the transmitter nodes and the A-scan is the average of the displacements over these nodes. In these studies, temperature effects were not considered. Normal (to the axis) input excitation was provided at one end of the helical waveguide as shown in Figure 2(b), in the form of a six ( $n=6$ ) cycle Hanning pulse displacement amplitude ( $A$ ), using the relationship in Equation (3)

$$\text{Hanning pulse (A)} = [1 - \cos(2\pi ft/n)] \cdot \cos(2\pi ft), \quad (3)$$

$$\text{Wave Length } (\lambda) = \frac{\text{Longitudinal velocity of waveguide (V}_L)}{\text{Input Frequency (f)}}, \quad (4)$$

$$\begin{aligned} \text{Mean diameter of the helical waveguide (D)} &= a\lambda; \\ (a &= 0.78 \text{ to } 3.12) \end{aligned} \quad (5)$$

$$\begin{aligned} \text{Total length of the wire (L)} &= \pi DN \quad (N = 1, 2, \dots) \\ \text{for un-constrained ends} \end{aligned} \quad (6a)$$

$$\begin{aligned} \text{Total free length of the helical waveguide (l)} &= \pi DN \tan \psi \\ &= L \tan \psi \end{aligned} \quad (6b)$$

where  $\psi$  is the pitch angle.<sup>28</sup>

$$\begin{aligned} \text{Pitch of the helical waveguide (P)} \\ &= \frac{\text{Free length of helical waveguide (l)}}{\text{Number of turns (N)}}. \end{aligned} \quad (7)$$

The longitudinal  $L(0, 1)$  mode A-scan signals that represent the free far end reflections in waveguides without any embodiments (notches) using pulse-echo mode were observed for the different dimensions of the helical waveguides (with varying  $D$  and  $P$  values) as shown in Figure 2(b). The waveguide wire diameter was maintained at

TABLE I. Material properties and helical waveguide parameters for finite element simulation.

Material	Mass density, $\rho$ (Kg m <sup>-3</sup> )	Young's modulus, E (GPa)	Poisson ratio, $\mu$	Element size (mm) & type	L, d in (mm)	Mean dia, D (mm)	Free length, l (mm)	No. of cycle (n), Freq (f, Hz)
Chromel	8650	214	0.3	$\lambda/28$ , 8-node brick	975, 1.18	0.78 $\lambda$ –3.12 $\lambda$	12.5, 50, 80	6, 400 $\times$ 10 <sup>3</sup>

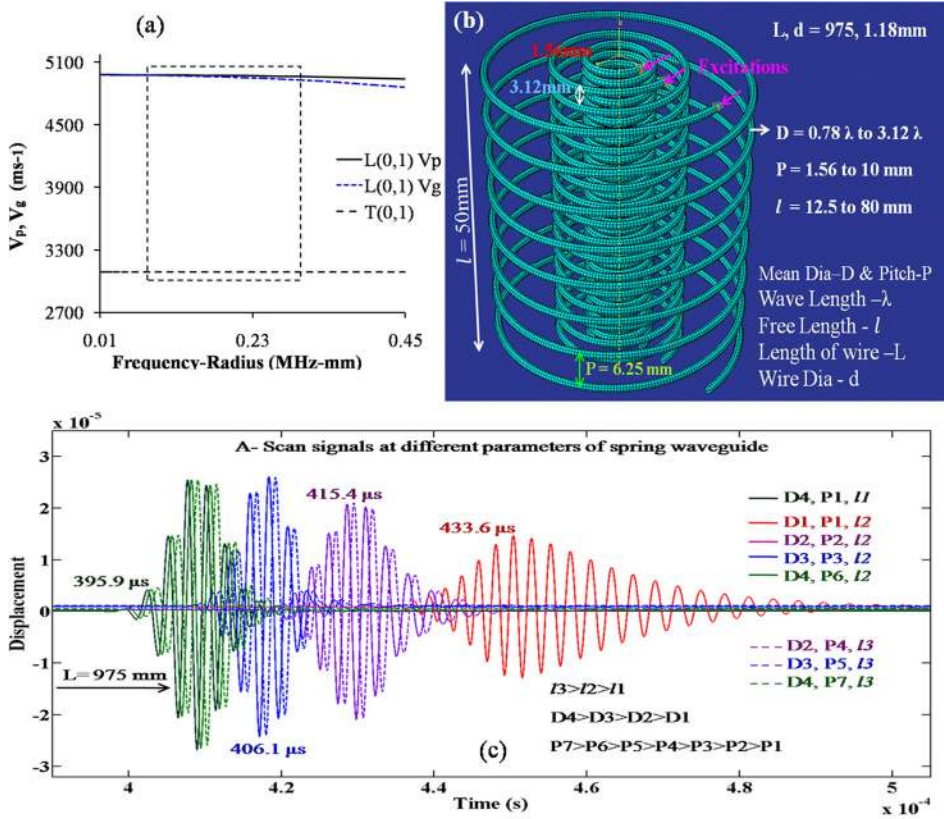


FIG. 2. (a) Dispersion curves (Phase velocity- $V_p$  and Group velocity- $V_g$ ) for a straight Chromel wire. (b) Helical waveguide dimensions at different parameters. (c) A-scan of the far end reflected signals obtained in pulse echo mode at different  $D$ ,  $P$ , and  $l$  values listed in Table II.

TABLE II. TOF and group velocity ( $V_g$ ) obtained using FEM simulation for different spring parameters.

D, P, l	Dimensions (mm)	No. of turns	TOF ( $\mu\text{s}$ )	$V_g$ (m/s)
D4, P1, l1	38.8, 1.56, 12.5	8	395.9	4929
D1, P1, l2	9.7, 1.56, 50	32	433.6	4501
D2, P2, l2	13.5, 2.17, 50	23	415.4	4698
D3, P3, l2	19.4, 3.12, 50	16	406.1	4806
D4, P6, l2	38.8, 6.25, 50	8	396.4	4919
D2, P4, l3	13.5, 3.48, 80	23	416.4	4683
D3, P5, l3	19.4, 5.00, 80	16	406.9	4793
D4, P7, l3	38.8, 10.0, 80	8	397.2	4910

1.18 mm and total nominal wire length ( $L$ ) of 975 mm. However, the  $L$  depends on the pitch angle  $\psi$  and can be calculated from Eq. 6(b). The corresponding TOF arrivals, and dimensions are marked in the A-scan plots. Significant change in  $L(0, 1)$  mode group velocity ( $V_g$ ) and different levels of dispersion were observed due to a change in mean coil diameters of the helical waveguide (ref: D1P1/2 and D4P1/1 in Fig. 2(c)). It was observed that as the mean coil diameter decreased, the group velocity decreased and the signal were observed to be relatively more dispersive in nature. For instance, when the  $D$  increased from 9.7 mm to 38.8 mm, the time of flight of the signal reflected from the far end of the waveguide decreased by 37.7  $\mu\text{s}$ .

A very small change in velocity was observed with the change in pitch  $P$  of the helical waveguide while keeping  $D$  a constant (ref: D4P1/1 and D4P7/3 in Figure 2(c)). For instance, for  $D = 38.8\text{mm}$ , a change in time of flight ( $\delta\text{TOF}$ ) caused by the change in the group velocity in the waveguide

was 1.30  $\mu\text{s}$  for a change of pitch from 1.56 mm to 10 mm and the corresponding change in the group velocity was 19 m/s. This change is due to two reasons, the first one is due to the slight change in total length due to strain induced by different helix angle (which is expected to be 0.1–0.2%) in the range of angles used here, and the second one is due to mild dispersion effects caused by the curvature changes. Both effects were found to be relatively small when compared to the relatively large  $\delta\text{TOF}$  caused by a change in  $D$ . Hence, it is observed that the wave propagation behaviour is more significantly influenced by the selection of the mean coil diameter and it is recommended that  $D$  must be carefully selected. However, the pitch of the helix (effect of stretching) is relatively less significant and hence the helix can be used as a reconfigurable sensor and the spacing between two levels of measurement can be configured by changing the  $P$ . The effect of change in  $P$  on the sensitivity of the measurement will be discussed in later in this section. From these results, the following observations can be summarized as below:

- The dispersive nature of wave propagation in a helical waveguide embodiment is dependent on mean coil diameter (due to stiffness effect), excitation frequency (wavelength- $\lambda$ ), and velocity of the material.
- The modes are more dispersive in nature when the mean coil diameter is  $< \lambda$ , and the change in group velocity, due to change in the pitch of the helix, was relatively small.
- Similar conclusions have been reported in the study using SAFE method.<sup>25</sup> In this work, the influence of pitch (defined as lay angle in the reference) was found to be less significant compared to the mean helix

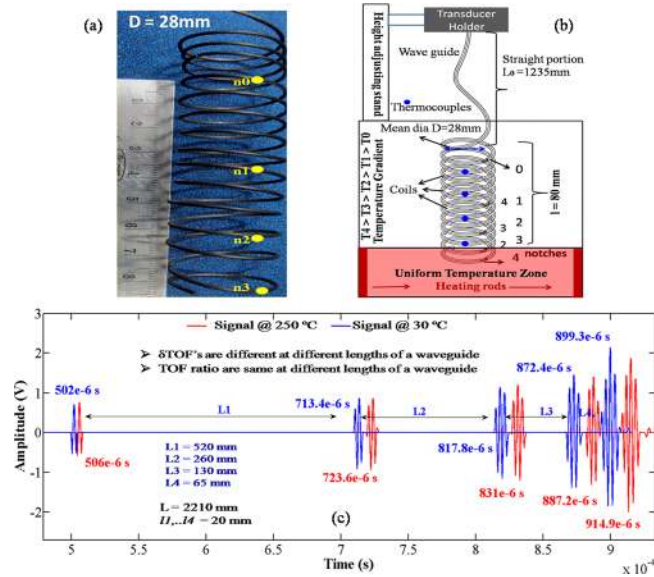


FIG. 3. (a) Photograph of Chromel helical waveguide with notches. (b) Schematic diagram of multiple notches (sensors) in a helical waveguide system with melter. (c) Reflected signals as received from the 4 notches and the end of the helical waveguide at different temperatures.

diameter. They also reported on some cut-off bands where the mode becomes non-propagating.

- (d) The optimal frequency-radius of wire has been chosen based on the non-dispersive region of the modes of interest as shown in Figure 2(a). The  $L(0, 1)$  mode wavelength was chosen to be less than the mean coil diameter of helical waveguide.
- (e) A more detailed FEM analysis of the helix parameters is beyond the scope of this paper, since the key interest here is to evaluate the feasibility of developing reconfigurable sensor for temperature measurement.

## IV. RESULTS AND DISCUSSION

### A. Experimental apparatus description

The diagram in Figure 3(a) describes the apparatus used in the experimental work reported here for temperature measurements at multi-levels in a high temperature test furnace. A similar experimental setup, procedure, apparatus, and transducer holder was described earlier in the literature.<sup>1,15–17,27–29</sup> Some preliminary experimental results using this spring-like sensing and comparison with a bank of straight waveguides has been reported previously.<sup>29</sup>

Multiple notches were machined along the length of the Chromel helical waveguide as shown in Figures 3(a) and 3(b). Here, the two key parameters are the mean helix diameter  $D$  and coil pitch  $P$  as described earlier. The axial spacing between the notches can be then adjusted by varying the pitch ( $P$ ), and consequently the helix angle is altered. In this system (Figure 3(a)) multiple notches were positioned in a helical spring in order to avoid the overlapping of signals from each notch as shown in Figure 3(c).

The ultrasonic pulse-echo mode was used (pulse/receiver, Olympus 5077) and the piezoelectric crystal based broadband ultrasound longitudinal (Panametrics/Olympus

NDT V101) transducers coupled the ultrasonic waves into the waveguide using a very thin layer of viscous Silicone based ultrasonic couplant. The longitudinal wave transducer was acoustically coupled to one end of the waveguide as shown in Figure 3(b) where the face of the transducer is normal to the axis of the waveguide during generation and reception. An 8 bit, 100 MHz sampling rate analog to digital converter was used to acquire and archive the A-scan signals that was supplied by the ultrasonic pulser-receiver in a Personal Computer (PC). Multiple reflected signals from multiple notches were continuously monitored using that signal peak-tracking technique method that has been described elsewhere.<sup>1</sup> The peak tracking approach ensured that the specific portion of the signals was tracked during the heating and cooling cycle to ensure the reliability of the TOF measurements, even though the signals shift during the heating process as shown in Figure 3(c). Subsequently, the  $\delta\text{TOF}$  between each pair of notches (one sensor) was measured using Equation (8). The TOF's and the  $\delta\text{TOF}$ 's of multiple notches (gage lengths) in the waveguide were recorded at different temperatures in furnace. The temperature was measured using calibrated reference thermocouples TC (K-type thermocouples), that were co-located in-between each notch position, during this initial calibration procedure. The surface temperatures of the transducers were both verified during each experiment to be the same as ambient temperature and was measured using a pyrometer. This is expected since the surface area of the waveguide is sufficiently high and the heat transfer along the length of the waveguide is negligible.

Instantaneous time of flight difference ( $\delta\text{TOF}$ ) of a waveguide is defined as below

$$(\delta\text{TOF}_{n+1})_i = [((\text{TOF})_{(n+1)i} - \text{TOF}_{ni}) - ((\text{TOF})_{(n+1)} - \text{TOF}_n)] \quad (8)$$

where  $\text{TOF}_{ni}$ ,  $\text{TOF}_n \rightarrow$  are defined as the instantaneous (i) TOF at various temperature and (ii) TOF at room temperature from each notch location  $n$ ,  $(\delta\text{TOF}_{n+1})_i \rightarrow$  are defined as the instantaneous change in TOF between the reflections from each sensor location  $n$

$$\frac{(\delta\text{TOF}_{n+1})_i}{\delta\text{TOF}_{n+1}} = \varepsilon_u, \quad (9)$$

where  $\varepsilon_u$  = Instantaneous ultrasonic TOF ratio.

### B. Case study 1, multiple sensors calibration and measurement in a uniform temperature region

Three Case studies using the helical waveguide system will be used for the calibration of waveguide followed by demonstration of multi-level temperature measurements. A special adjustment fixture apparatus was used to control the pitch of the waveguide. In case study 1, a free length  $l = 80$  mm of Chromel (1.18 mm diameter) helical waveguide with 4 sensor embodiments was used (made of 4 notches); each sensing region was kept at 20 mm spacing by adjusting (using adjuster) the pitch between notches as shown in Figure 4(a). In this case,

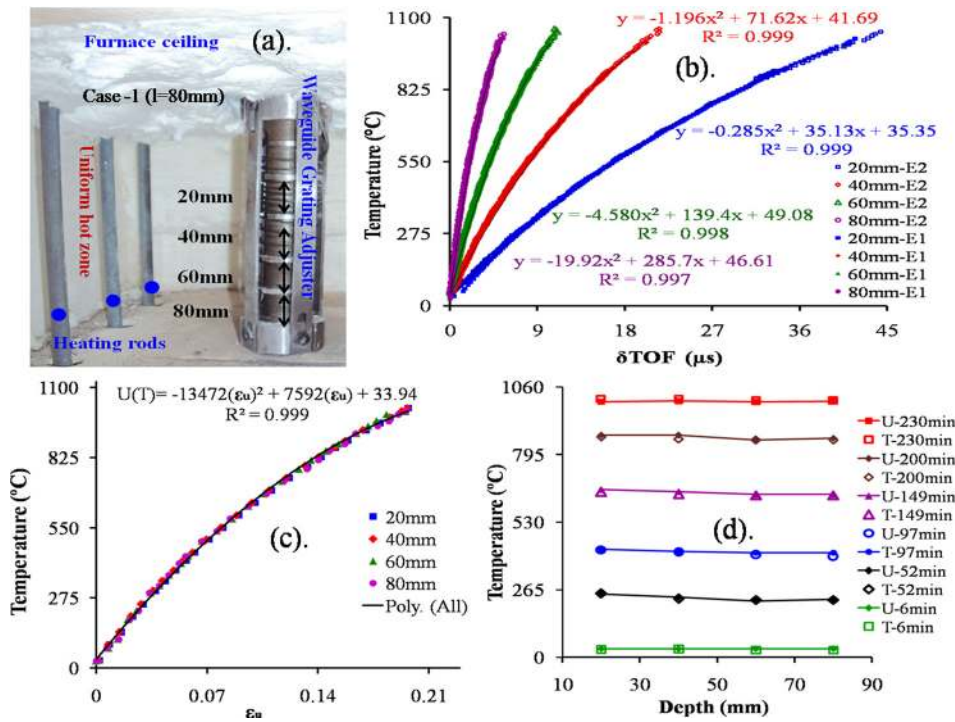


FIG. 4. (a) Shows the multiple-sensors of a helical waveguide at uniform temperature zone in the furnace. (b) The  $\delta\text{TOF}$ 's of each notch sensors at various temperatures. (c)  $\epsilon_u$  vs Temperature for all notches representing the calibration curve. (d) Comparison of temperature measurement using ultrasonic waveguide method (solid) with thermocouple (hollow).

the entire helical waveguide system was positioned in the uniform temperature region inside the furnace.

For each sensor,  $\delta\text{TOF}$  was measured using Equation (8), from a helical waveguide as in Figure 4(a) at uniform hot zone, and the corresponding temperature was monitored using collocated thermocouples. The  $\delta\text{TOF}$  vs temperature curves from each sensor followed a different slope from two separate heating experiments (E1 and E2) as shown in Figure 4(b). In this paper, our scope was to achieve single calibration curve for measuring the temperature for all the temperature zones. When all the TOF ratio ( $\epsilon_u$ ) from all the notches were plotted as a

function of temperature, it is observed that a single calibration curve was obtained as shown in Figure 4(c). This calibration curve relates measured TOF ratio  $\epsilon_u$  as defined by Eq. (9) for any sensor to the surrounding temperature. If the temperature (T) is in Celsius and  $\epsilon_u$  is dimensionless, the 2nd order polynomial expression for this curve was found to be as given below

$$T = -13472(\epsilon_u)^2 + 7592(\epsilon_u) + 33.94. \quad (10)$$

Using this expression in Equation (10), the temperatures were computed at each sensor location using  $\epsilon_u$ . The

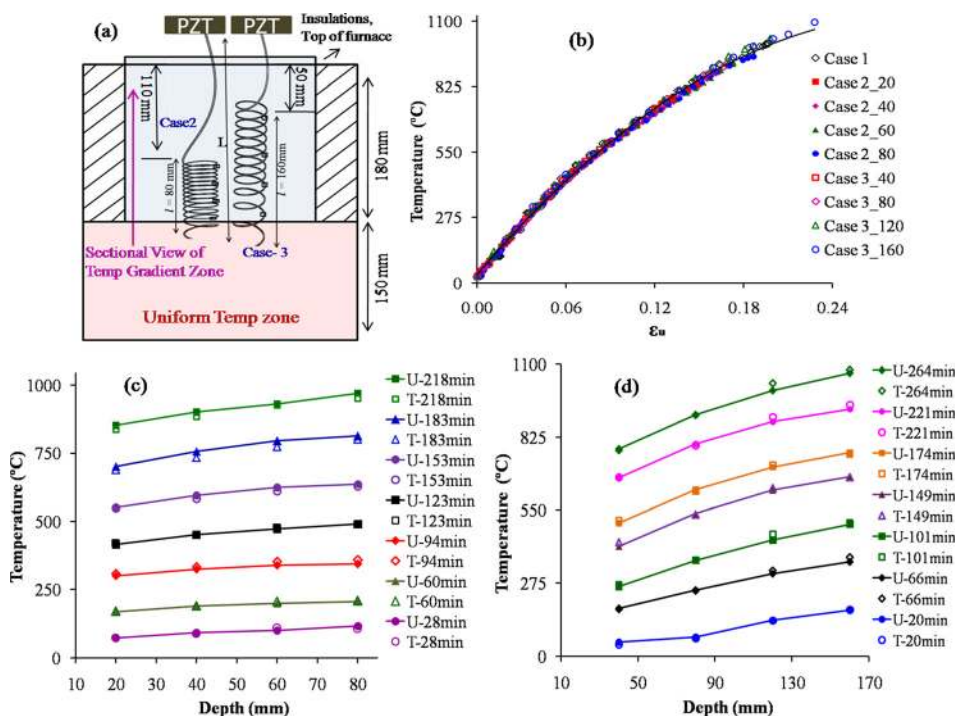


FIG. 5. (a) Multiple sensors of a helical waveguide at insulated region of the furnace. (b) Multiple sensors waveguide calibration from 160 mm depth of temperature gradients. (c) Ultrasonic and thermocouple measurements from different depths at different time instances using 80 mm free length of helical waveguide. (d) Ultrasonic and thermocouple measurements from different depths using 160 mm free length.

temperatures thus obtained were compared with the thermocouple measurements and plotted in the same graph for a typical 4 hr heating cycle of the furnace as shown in Figure 4(d). As expected, the two methods were found to compare well, with a maximum average error of 1–3 °C. The result in Figure 4(d) shows that the polynomial fit calibration curve in Equation (10) is acceptable to be used for the waveguide based measurement of temperature.

This helical sensor waveguide system was then used to measure the temperature at different time instances in zones in the furnace with temperature gradients as discussed in cases 2 and 3 explained below.

### C. Case studies 2 and 3, multi-level temperature measurement in non-uniform temperature region

In case studies 2 and 3, the Chromel helical waveguides were positioned in the insulated region of the furnace as shown in Figure 5(a) where the temperature varied from the uniform temperature zone to the external wall of the furnace. Like before, K type thermocouples were co-located in between each notch position. Two length configurations of the helix waveguide were demonstrated with  $D = 28$  mm, but with different pitch and consequently different free length ( $l$ ) of the helix.

In case study 2, a free length  $l = 80$  mm with 4 notches at 20 mm spacing (along the free length positioned at 20, 40, 60, 80 mm from the bottom of the insulation) and in case study 3, a free length  $l = 160$  mm with 40 mm notch spacing (at 40, 80, 120, 160 mm from the bottom of the insulation) were used. In both the case studies, the same waveguide was used and the free length was adjusted to the required length by adjusting the pitch between notches using the fixture introduced earlier in Figure 4(a). The bottom most notch was positioned closer to the bottom of the insulation, in proximity to the uniform temperature region. Figure 5(a) illustrates the positions and approximate notch configurations of these two case studies.

Steady state of heating experiments were conducted for both the case studies and the  $\delta$ TOF data (using Eq. (8)) were collected from all sensor locations (notches) at a time interval of 60 s. The  $\epsilon_u$  values as well as the temperature at the co-located thermocouples, from the 4 sensor locations were measured at different temperatures inside the furnace.

In Figure 5(b), the  $\epsilon_u$  vs temperature measured using the thermocouples are plotted for all the 3 case studies, that is, including the earlier case where the entire waveguide was inside the uniform gradient region. This plot shows that the calibration curve obtained earlier is applicable to the temperature gradient cases also and Equation (10) obtained earlier may be used for this data set. In Figures 5(c) and 5(d), the temperatures measured using the ultrasonic waveguide (U) is compared with the thermocouple reading (T) for the 4 locations at different time instances of measurements. It may be observed from these results that the ultrasonic waveguide technique can be used for measuring the temperature in a region with varying temperature and the relative differences between the two reading is relatively small. The maximum difference between the ultrasonic and the thermocouple was

9 °C and the average error was less than 1.6 °C with a standard deviation of 0.5 °C. These two case studies also demonstrated the re-configurable nature of the helix waveguide.

As previously mentioned, change in  $P$  will affect the  $V_g$  of the ultrasonic guided wave, albeit to a small extent. For the two extreme  $P$ 's considered in Table II, the change in  $\epsilon_u$  due to the change in the pitch (at room temperature) was of the order of 0.0038. This effect will result in an error of the order of 0.38% in the measurements. Since  $V_g$  can be predicted for different helix lengths<sup>30</sup> using the FEM model, a correction factor may be introduced for compensation of this effect. However, as can be concluded from Figures 5(c) and 5(d), the effect of the change in group velocity due change in  $P$ , within the range considered, can be assumed to be negligible.

## V. CONCLUSIONS

A novel ultrasonic reconfigurable temperature sensor mechanism and sensing principle is described here which provides a more robust and cost effective solution for measurement of temperature gradients, in applications involving elevated temperature processes, when compared to junction based thermocouples. This novel technique uses multiple notches that define the gage lengths for the sensors that can be re-positioned by varying the free length (consequently the pitch) of the helical waveguide. This ultrasonic waveguide sensor employs the guided  $L(0, 1)$  mode that can be reliably generated and received by using a conventional longitudinal transducer. Using a 3D FEM simulation study, it was determined that the mean helix diameter has significant effect on the wave propagation while the pitch of the helix is relatively negligible. Hence, using a helical waveguide and by adjusting the pitch, the gage lengths of the sensing regions can be varied. Using the TOF ratio  $\epsilon_u$  and using a calibration curve obtained experimentally, it was demonstrated here that temperatures could be measured reliably at multiple levels in temperature gradient regions inside a furnace using a single waveguide.

In this paper, the material used was Chromel, due to its availability and high temperature properties. However, other materials such as Kanthal, Stainless Steel, and Platinum may also be used. In this work, only 4 notches were used. It must be feasible to increase the number of sensors, but may depend on the material and its ability to sustain the guided ultrasonic waves. The experimental calibration curve was critical for the calculation of the local temperature.

## ACKNOWLEDGMENTS

The authors wish to thank the Board for Research in Nuclear Sciences (BRNS), Mumbai, INDIA, for financial support for this work.

<sup>1</sup>S. Periyannan and K. Balasubramaniam, *Measurement* **61**, 185 (2015).

<sup>2</sup>V. V. Shah and K. Balasubramaniam, *Ultrasonics* **34**(8), 817 (1996).

<sup>3</sup>K. Balasubramaniam, V. V. Shah, G. Boudreaux, R. D. Costley, C. Menezes, and J. P. Singh, *Rev. Prog. Quant. Nondestr. Eval.* **18B**, 1163 (1999).

<sup>4</sup>K. Balasubramaniam, V. V. Shah, D. Costley, G. Bourdeaux, and J. P. Singh, *Rev. Sci. Instrum.* **70**(12), 4618 (1999).

- <sup>5</sup>K. Balasubramaniam, V. V. Shah, D. Costley, G. Bourdeaux, and J. P. Singh, U.S. patent 6,296,385 (2 Oct 2001).
- <sup>6</sup>V. V. Shah and K. Balasubramaniam, *Ultrasonics* **38**, 921 (2000).
- <sup>7</sup>V. S. K. Prasad, K. Balasubramaniam, E. Kannan, and K. L. Geisinger, *J. Mater. Process. Technol.* **207**, 315 (2008).
- <sup>8</sup>R. D. Costley, K. Balasubramaniam, W. M. Ingham, J. A. Simpson, and V. Shah, *Rev. Prog. Quant. Nondestr. Eval.* **17**, 859 (1998).
- <sup>9</sup>J. C. Pandey, M. Raj, S. N. Lenka, S. Periyannan, and K. Balasubramaniam, *J. Iron Making Steel Making* **38**, 74 (2011).
- <sup>10</sup>C. K. Jen, K. Y. Thanh Nguyen, B. Cao, H. Wang, and C. A. Loong, U.S. patent 5,951,163 (14 Sep 1999).
- <sup>11</sup>R. B. Bentley, *Sens. Actuators, A* **24**, 21 (1990).
- <sup>12</sup>K. N. Huang, C. F. Huang, Y. C. Li, and M. S. Young, *IEEE EMBS Asian-Pacific Conference on Biomedical Engineering* (2003), p. 294.
- <sup>13</sup>W. Y. Tsai, H. C. Chen, and T. L. Liao, *Sens. Actuators, A: Physical* **132**, 526 (2006).
- <sup>14</sup>T. S. Zhan, S. L. Wu, and W. Y. Tsai, *J. Sci. Ind. Res.* **68**, 44 (2009).
- <sup>15</sup>S. Periyannan and K. Balasubramaniam, "Temperature dependent E and G measurement of materials using ultrasonic guided waves," *AIP Conf. Proc.* **1581**(1), 256 (2014).
- <sup>16</sup>S. Periyannan and K. Balasubramaniam, "Temperature gradients and material properties measurements using Ultrasonic guided waves," European Conference on Non-Destructive Testing, Prague, Czech Republic, 6–10 October 2014.
- <sup>17</sup>K. Balasubramaniam and S. Periyannan, "A novel waveguide technique for the simultaneous measurement of temperatures dependent properties of materials," Patent number (World Intellectual Property Organization, 2015), WO 2015/008299A2.
- <sup>18</sup>P. Cawley and F. B. Cegla, U.S. patent 8,381,592 (26 Feb 2013).
- <sup>19</sup>W. K. Spratt and J. F. Vetelino, *IEEE International Frequency Control Symposium, 2009 Joint with the 22nd European Frequency and Time forum* (2009), p. 850.
- <sup>20</sup>E. Vargas, R. Ceres, J. M. Martin, and L. Calderon, *Sens. Actuators, A: Physical* **61**, 256 (1997).
- <sup>21</sup>K. Visvanathan and K. Balasubramaniam, *Rev. Sci. Instrum.* **78**, 015110 (2007).
- <sup>22</sup>J. L. Rose, *Ultrasonic Waves in Solid Media* (Cambridge University Press, Cambridge, UK, 1999), pp. 143–152.
- <sup>23</sup>B. N. Pavlakovic, M. J. S. Lowe, P. Cawley, and D. N. Alleyne, "DISPERSE: A general purpose program for creating dispersion curves," *Rev. Prog. Quant. Nondestr. Eval.* **16**, 185 (1997).
- <sup>24</sup>S. Ahn and A. K. Ganguly, *IEEE Trans. Electron Devices* **ED-33**(9), 1348 (1986).
- <sup>25</sup>F. Treysse, *Wave Motion* **45**, 457 (2008).
- <sup>26</sup>S. Periyannan and K. Balasubramaniam, *AIP Conf. Proc.* **1430**(1), 1655 (2012).
- <sup>27</sup>S. Periyannan and K. Balasubramaniam, *Rev. Sci. Instrum.* **86**, 114903 (2015).
- <sup>28</sup>W. Sollfrey, *J. Appl. Phys.* **22**, 905 (1951).
- <sup>29</sup>S. Periyannan, K. Balasubramaniam, and P. Rajagopal, *Phys. Procedia* **70**, 514 (2015).
- <sup>30</sup>F. Treysse and L. Laguerre, *J. Sound Vibration* **329**, 1702 (2010).